Chemical Papers (2020) 74:3767–3783
https://doi.org/10.1007/s11696-020-01196-0

REVIEW

Synthetic routes of the reduced graphene oxide

Jianlang Feng[1] · Yunqing Ye[1] · Meng Xiao[2] · Gang Wu[3] · Yu Ke[1]

Received: 26 October 2019 / Accepted: 12 February 2020 / Published online: 22 May 2020

Abstract
Graphene has attracted great attention owing to its exceptional electrical, mechanical, optical, thermal and antimicrobial properties. Graphene oxide (GO) and reduced graphene oxide (rGO) are two important derivatives of graphene, and the latter can be achieved through the reduction reaction of GO. Many methods including reductant reduction, irradiation reduction, electrochemical reduction and microbial reduction were summarized systematically, with an aim at obtaining superior rGO and even rGO-based devices on a large-scale production. The latest development of different strategies on the reduction of GO and their relevant mechanism were reviewed as a guide for further studies of rGO.

Keywords Graphene oxide · Reduced graphene oxide · Reduction mechanism · Patterning

Introduction

Graphene is a sp^2 hybridized carbon atoms densely arranged in two-dimensional hexagonal lattice with a 0.142-nm carbon–carbon bond length (Singh et al. 2011). Since being exfoliated from highly oriented pyrolytic graphite by Novoselov et al. (2004), graphene nanosheets have been mass produced through several exfoliation processes, destroying Van der Waals' force between layers via gas (Wu et al. 2018), liquid (Amiri et al. 2018), electrical discharge (Segundo et al. 2018) and ultrasound exfoliation (Navik et al. 2018; Balasubramaniam and Balakumar 2016). Graphene and its derivatives have attracted close attention due to their unique morphologies and extraordinary electrical, mechanical, optical, thermal and antimicrobial properties (Soldano et al. 2010). These fascinating materials have been proposed to be used in semiconductor, sensors, energy storage and medical areas (Huang et al. 2011; Traversi et al. 2013; Kamat 2009). For example, graphene is very promising in bone scaffold due to its biocompatibility and capability of differentiating human mesenchymal stem cells into bone cells without hampering their proliferation (Nayak et al. 2011). It is also an excellent adsorbent for removing heavy metals owing to its large specific surface area (Elgengehi et al. 2020). Graphene or its nanocomposites with metal, metal oxide, metal salt and nonmetallic elements play an important role in fuel cells, supercapacitors and solar cells areas (Tsang et al. 2020; Balasubramaniam and Balakumar 2017a, b). Optical devices based on graphene exhibit good refractive index and optical transparency in the visible light range (Zhang et al. 2010a, b). High photo-thermal conversion capacity makes graphene be promising responsive materials for phototherapy, flexible photonic and electronic devices, and smart windows photodetectors (Chi et al. 2019).

Graphene oxide (GO, Fig. 1), one derivative of graphene, is heavily decorated with a series of oxygen-containing groups such as hydroxyl, carboxyl, epoxy and ketone along the carbon atoms. The common methods for chemical preparation of GO and their features were listed in Table 1. Graphite was exfoliated chemically by potassium chlorate and fuming nitric acid via Brodie method (Brodie 1859). Staudenmaier (1898) used sulfuric acid instead of two-third of fuming nitric acid and multiple aliquot of potassium chlorate in the reaction, but the obtained graphite layers were often damaged. In Hummers method, graphite was oxidized

✉ Gang Wu
imwugang@scut.edu.cn

✉ Yu Ke
lisa6863@163.com

[1] Department of Biomedical Engineering, Key Laboratory of Biomaterials of Guangdong Higher Education Institutes, College of Life Science and Technology, Jinan University, Guangzhou 510632, China

[2] Department of Materials Science and Engineering, School of Chemistry and Materials, Jinan University, Guangzhou 510632, China

[3] Department of Biomedical Engineering, South China University of Technology, Guangzhou 510641, China

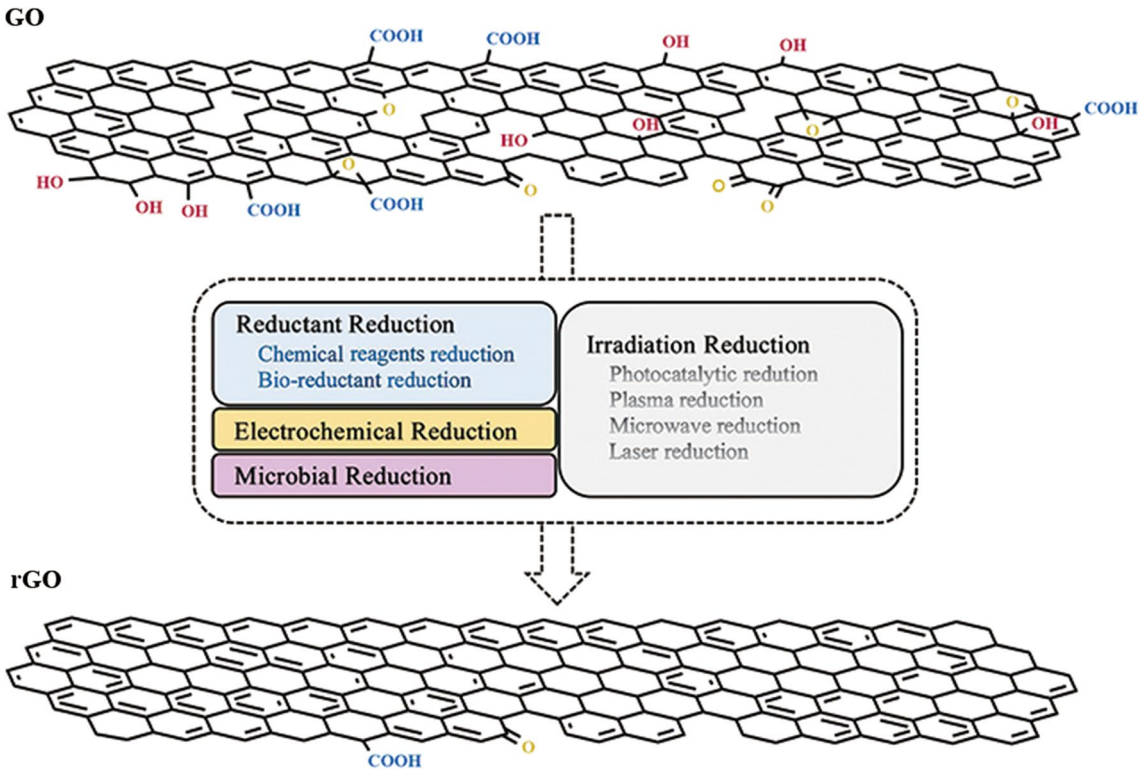

Fig. 1 Schematic reduction method of graphene oxide

Table 1 Chemical methods for preparing GO

Methods	Reaction condition	Features	References
Brodie method	Mixed graphite and $KClO_3$ at a ratio of 1:3 Reacted with HNO_3 for 3–4 days at 60 °C	Higher degree of oxidation Long reaction time, explosive characteristics of $KClO_3$ and releasing toxic gas	Brodie (1859)
Staudenmaier method	Mixed fuming HNO_3 and concentrated H_2SO_4 at a ratio of 1:3 Reacted with graphite in an ice bath Added $HClO_4$ slowly to the mixture for 4 d	Higher degree of oxidation Long reaction time, explosive characteristics of $KClO_3$ and releasing toxic gas Damaged the structure of graphite layers	Staudenmaier (1898)
Hummers method	Mixed $NaNO_3$ and graphite at a ratio of 1:2 Reacted with concentrated H_2SO_4 at 0 °C for 15 min Reacted with $KMnO_4$ and cooled for 15 min Stirred for 1 h and added water for 10 min Added 30% H_2O_2 until bright yellow color	Much safer Relatively low degree of oxidation than modified Hummers method Emitting toxic gas	Hummers and Offeman (1958)
Modified Hummers method	Similar to Hummers method Replaced $NaNO_3$ with H_2SO_4 and H_3PO_4 Added double amount of $KMnO_4$	Low exotherm No toxic gas More hydrophilic carbon material	Marcano et al. (2010)

by concentrated sodium nitrate and potassium permanganate (Hummers and Offeman 1958) in a few hours to produce GO. It is a very common method with various oxidization conditions (Wu et al. 2009; Zhao et al. 2010), but toxic gas

such as NO_2 and N_2O_4 was produced. Graphites oxidized by Hummers method had a high oxygen contents and large interlayer distances than the above methods (Muzyka et al. 2017). The oxygen moieties were also easier to remove upon thermal annealing than those by the other methods, showing a better electrochemical performance (Botas et al. 2013; Poh et al. 2012). The modified Hummers method being developed by Marcano et al. (2010) employed double amount of potassium permanganate and sulfuric acid/phosphoric acid to replace sodium nitrate. It produces more hydrophilic carbon material without toxic gas and large exotherm than Hummers method. The parameters of the oxidation reaction, such as potassium permanganate amount, oxidation temperature and time, influenced the oxygen contents and interlayer spacing of GO, providing different chemical or physical structure even after GO was reduced (Kavimani et al. 2017; Trenczek-Zajac et al. 2016).

GO can be converted into the reduced graphene oxide (rGO, Fig. 1) via removing oxygen-containing groups, showing quite different properties in some respects. For example, the hydrophobic rGO is prone to aggregation to change its characteristics such as shape and specific area, but the oxygen-containing groups enhance the hydrophilicity greatly and make GO more stable in water (Stankovich et al. 2006). It is still a controversial to conclude which one possesses better antibacterial capacity (Zou et al. 2016). However, rGO demonstrates better chemical stability and electronic conductivity, with the resistance ranges of (5–500) GΩ cm and (100–1000) Ω cm, respectively, for GO and rGO (Pei and Cheng 2012; Xu et al. 2018; Becerril et al. 2008). These features have appealed continuous studies on the performance of rGO and opened exciting new opportunities for applications of rGO and rGO-based device in many areas.

Many methods have recently been proposed to prepare rGO, with different residue groups and structural defects to ultimately affect their function. Low energy consumption and non-toxicity process have been two main focuses for the synthesis of rGO, especially for large-scale industrial production. This paper summarized the progress on the reduction method for GO and relevant reaction mechanism.

Reduction via reductant

Chemical reagents

Oxygen-containing groups of GO can be eliminated through a redox reduction with the reductive reagents. Reduction via common chemical reagents is the most traditional way to produce rGO, which has shown great potential in the large-scale production of graphene. Hydrazine hydrate possessed high reductivity to carbonyl groups, but nitrogen doping in the carbon lattice changed the conductive of rGO as well. The result proposed by Stankovich et al. (2007) showed that C/N ratio of rGO was 16.1 after the reduction by hydrazine hydrate for 24 h. Lin et al. fabricated N-dope few-layer mesoporous carbon with the conductive and specific capacitance of 360 S cm^{-1} and 790 F g^{-1} in 0.5 M H_2SO_4 electrolyte, respectively. The efficient reduction of GO and restoration of π–π conjugated network of sp^2 hybridized carbon structure presented advantages in the field of electronics (Lin et al. 2015). Sodium borohydride was more effective than hydrazine hydrate because no extra elements would be doped on the carbon planes. It reduced ketones to alcohol groups more easily than carbonyl and epoxy groups (Shin et al. 2009). The mixture of sodium borohydride and calcium chloride was reported to promote the elimination of the hydroxyl groups compared with sodium borohydride alone. The resulting rGO with a C/O ratio of 19.0 presented lower electrical resistance and high capacitance of 162 F g^{-1} in alkaline media and 164 F g^{-1} in acidic media (Yang et al. 2015). A two-step reduction strategy using sodium borohydride and hydrazine successively was applied to produce more conductive rGO than the ones by sodium borohydride or hydrazine alone, showing potential application as supercapacitors, batteries or sensors (Wei et al. 2017). Krishna et al. (2015) developed a method via using hydrazine hydrate and citric acid in an alkaline condition, and obtained more exfoliated rGO with better electrical property than the reductive one by hydrazine hydrate.

Hydroxylamine was proven to be an effective chemical reductant due to less toxic and explosive than hydrazine hydrate. rGO being reduced by hydroxylamine at 90 °C for 1 h possessed a C/O ratio from 2.0 to 9.8, in comparable to hydrazine hydrate reduction for 24 h. However, it showed more defect of carbon lattice than the ones by hydrazine or sodium borohydride (Yaragalla et al. 2017). Hydroiodic acid was applied to prepare flexible rGO film that showed higher C/O ratio and conductive capacity than those reduced by hydrazine hydrate and sodium borohydride, because the latter two released gas by-product to destroy the films. However, a small amount of iodine remained on the rGO films. Other halogenation agents including $SOCl_2$ and HBr were also reported to reduce GO in different levels (Pei et al. 2010), demonstrating the possibility of GO reduction in acidic condition.

Generally, the above chemical compounds are toxic and hazardous that will cause health risks or environmental pollutions. Therefore, non-toxic reductants including sodium oxalate (Hanifah et al. 2015), sodium acetate trihydrate (Zhang et al. 2014a, b) and dipotassium hydrogen phosphate (Zhang et al. 2013a, b) were employed to produce rGO in alkaline condition. Figure 2 illustrates the deoxygenation mechanism of various oxygen-containing groups of GO. Hydroxyl (Fig. 2a) was first protonated under sodium oxalate basic solution and converted into H_2O to form the

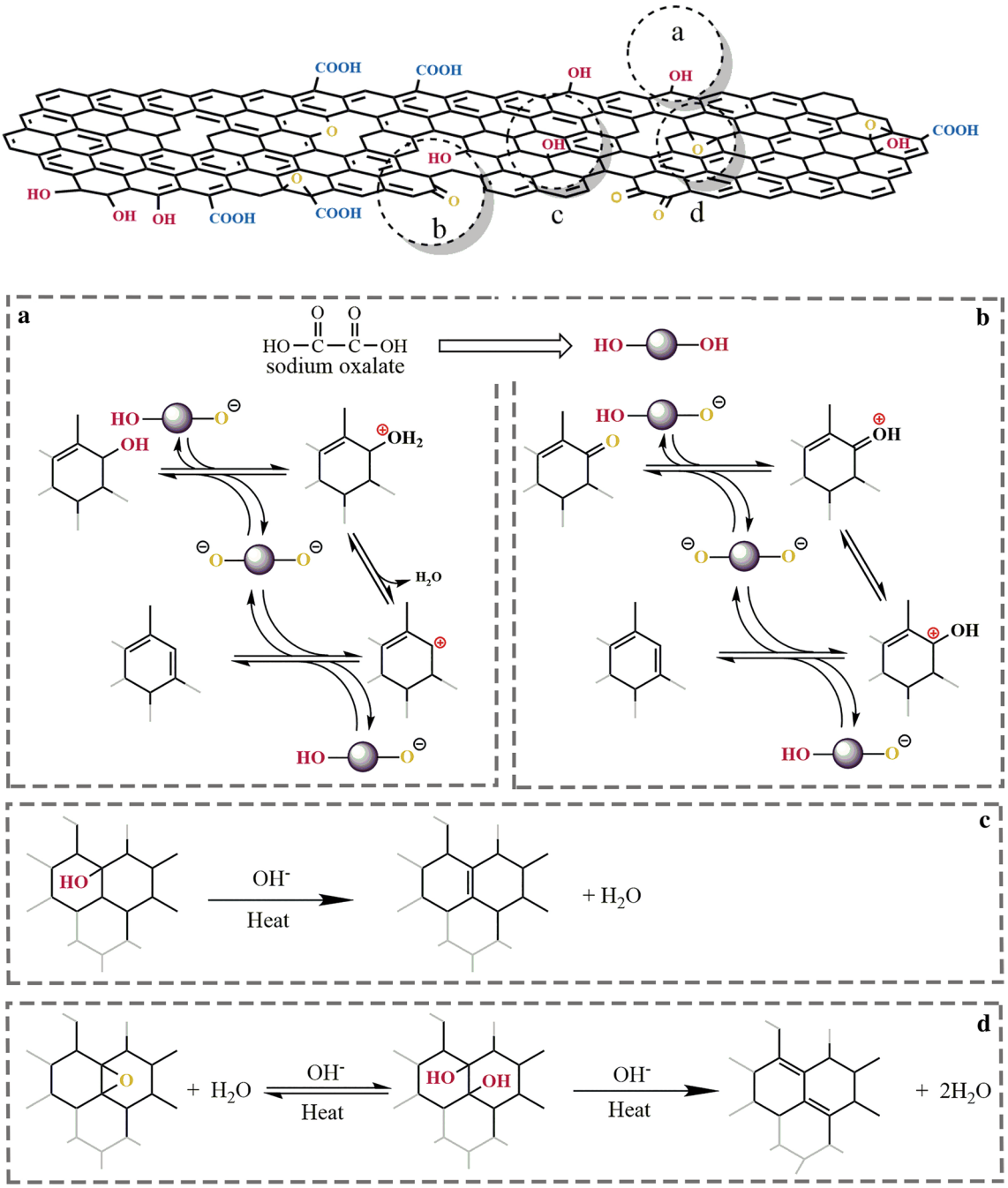

Fig. 2 Mechanism of chemical reduction: nucleophilic reaction of hydroxyl group (**a**) and carbonyl (**b**) by sodium oxalate (Hanifah et al. 2015), and dehydration reaction of hydroxyl group (**c**) and epoxy group (**d**) by sodium acetate trihydrate (Zhang et al. 2014a, b)

carbocation. The oxalate ions then abstracted the neighboring hydrogen of the carbocation to form double bonds. Carbonyl groups (Fig. 2b) can be protonated to form hydroxyl ions that were reduced in a similar mechanism mentioned above (Hanifah et al. 2015). Dehydration reaction was suggested as another solution to GO reduction. Sodium acetate trihydrate was hydrolyzed to produce alkaline environment, where hydroxyl groups could combine with its neighboring hydrogen atoms through dehydration reaction to produce rGO (Fig. 2c), or the epoxy groups (Fig. 2d) were hydrated and transformed into two hydroxyl groups that reduced further with the neighboring hydrogen to give H_2O (Zhang et al. 2014a, b). Ethanol, ethylene glycol and glycerol were also proven as precisely selective reductants of epoxy groups, while hydroxyl and carboxyl groups remained (Xu et al. 2014). These reductants showed poor reducing degree

though less hazardous than hydrazine hydrate, which would limit them from large-scale production.

GO can also be reduced by certain solvents in a sealed container above the boiling point without any additional reductants. *N*,*N*-dimethylformamide (solvent) was used to reduce GO at high temperature (120–200 °C) for 12 h and obtained rGO with the intensity ratio of D-Raman peak to G-Raman peak (I_D/I_G) increasing to 0.93. C/O ratio of rGO via solvothermal reduction at 180 °C was 5.52 compared to 2.02 of GO, and long reaction time facilitated to obtain rGO with high C/O atomic ratio (Zhou et al. 2011; Kim et al. 2016). The introduction of sulfuric acid (as catalysts) shortens the reaction time and enhanced the reaction efficiency. Only 1 h of reduction by solvent and catalysts produced rGO with high C/O ratio of 8.4 compared with 6.5 of solvent reduction (Tien et al. 2012). rGO via vinylpyrrolidone (solvent) reduction at 250 °C had the conductivity up to 1.38×10^3 S.m^{-1}, showing potential applications in solar cells or electromagnetic interference shielding of signal cables (Dubin et al. 2010). Since *N*,*N*-dimethylformamide and vinylpyrrolidone introduced nitrogen in the carbon lattice, mixed solvent of acetone and sodium hypochlorite was employed as the substitution to reduce GO at 120 °C for 2 h and obtained rGO with a C/O ratio of 8.23 and I_D/I_G ratio of 1.65 (Kim et al. 2014a, b). Though the mechanism of solvothermal reduction is still questionable, it is generally accepted that high pressure and temperature promote the deoxygenation of GO, where the solvents can behave as strong electrolytes to cleave the oxygen-containing bonds (Zhou et al. 2009; Chen et al. 2013). A green method based on refluxing aqueous GO suspension was designed to control oxygen contents, but C/O ratio only reached 6 after 7 d of reflux. Such long reduction time would limit its application in large-scale commercial production (Park et al. 2014).

In summary, the reduction of GO by chemical reductants can be realized at room temperature or by moderate heating, making it a cheap and easy way to produce stable dispersion of rGO sheets. Reductants like hydrazine hydrate and sodium borohydride are most commonly used because of their high effectiveness, but most of them are corrosive, explosive or hazardous. Much effort has been made to explore non-toxic reducing reagents as the substitutes, though most of them present lower reduction efficiency than traditional ones and are likely to aggregate due to strong π–π stacking tendency and Van der Waals' interaction among rGO sheets (Guo et al. 2011). Solvothermal reduction without extra chemical reductants is very promising; however, it often requires special equipment and rigorous condition.

Bio-reductants

Most chemical reagents are toxic and do not suitable for bio-related applications; therefore, economic and eco-friendly natural reductants have been considered. Amino acids contain many reactive groups on the main and/or side chains to react with GO, among which L-cysteine with the reductive thiol groups was the first amino acid for the reduction (Chen et al. 2011). Amine groups of alanine can also attack epoxy and hydroxyl groups of GO nucleophilically (Wang et al. 2017). Reducing sugars (glucose, fructose and sucrose) can form H-bond with oxygen-containing groups of GO and convert into lactone themselves (Zhu et al. 2010; Akhavan et al. 2012). L-Ascorbic acid was prone to be oxidized because of its strong reductivity (Zhang et al. 2010). During the reduction process (Fig. 3), ascorbic acid functioned as the nucleophile and attacked the hydroxyl (a) and epoxide (b) groups to release H_2O. The resulted intermediate underwent thermal elimination reaction, forming the double bonds on rGO and dehydroascorbic acid (Gao et al. 2010Ascorbic acid was also proven to produce a more stable rGO in the alkaline condition through electrostatic repulsion to inhibit rGO agglomeration (Xu et al. 2015). Recently, Hou et al. (2018) synthesized rGO using artemisinin in ethanol with a C/O ratio as high as 11.7, probably owing to the formation of an endoperoxide bridge. In general, the reduction degree via bio-reductants was lower than those of traditional chemical reagents, and the defects were introduced on carbon plane meanwhile.

Plant extraction has attracted much attention because it contains bioactive proteins, vitamins, amino acids, polyphenol and flavonoid that may act as the reducing or capping agents in the production of rGO. Therefore, reducing process via plant extract is very complicated. For example, bio-reduction via *eucalyptus leaf* involved 11 major biomolecules (Li et al. 2017; Jin et al. 2018). Hou et al. (2017) compared the plant extraction with common chemical reductant and found that rGO reduced by hydrazine hydrate displayed much smaller plates with obvious curled edges and the one by *Lycium barbarum* extract possessed more defects.

Polyphenols are a class of natural secondary metabolites characterized by the presence of polyatomic phenol, and existed largely in different parts of peels, roots, leaves and fruits. Seed extracts of *Terminalia chebula* were reported as green reductants to reduce the oxygen-containing groups and stabilized rGO solution by preventing aggregation as well (Maddinedi et al. 2015). Flavonoids are non-ketone polyhydroxy polyphenol compounds contained in different parts of plant, and also a class of plant secondary metabolites to perform many functions, such as flower coloration, chemical messengers, physiological regulators and cell cycle inhibitor (Galeotti et al. 2008). The degree of deoxygenation using *chrysanthemum* extract containing flavonoids (diosmetin, luteolin, apigenin and glucoside) was comparable to hydrazine hydrate (Hou et al. 2016). Polyphenols and flavonoids with oxygen anion and phenolic hydroxyl group can react with the epoxide moiety through a SN^2 mechanism to induce

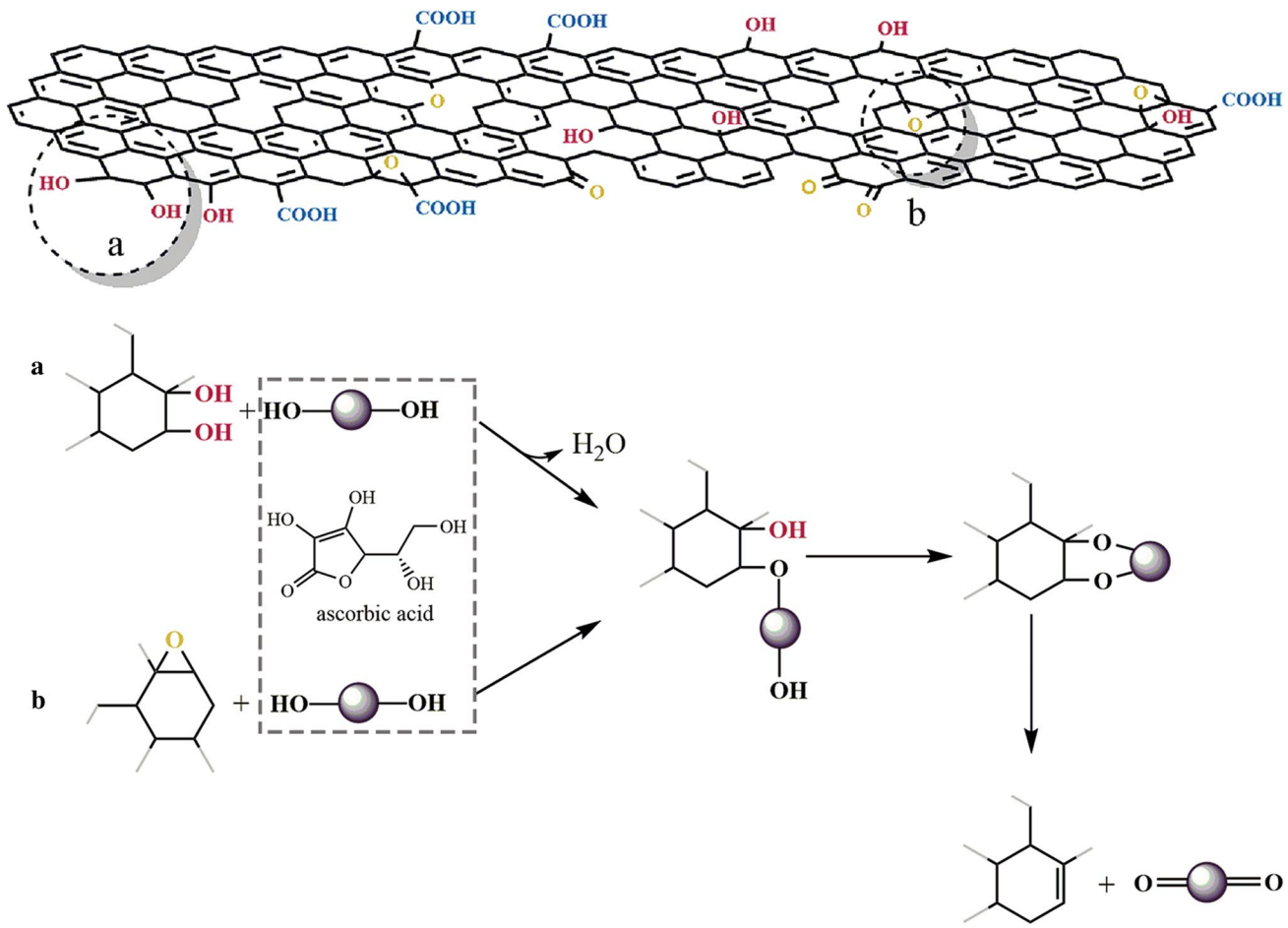

Fig. 3 Mechanism of the reduction process by ascorbic acid: (**a**) nucleophilic reaction of double hydroxyl group; (**b**) nucleophilic reaction of epoxy group (Gao et al. 2010)

the opening reaction of the oxirane ring, or attack carbonyl and hydroxyl groups through eliminating water molecules, resulting in the corresponding benzoquinone themselves (Thakur and Karak 2012; Sykam et al. 2018).

Nettle extract containing histamine and serotonin was an extremely effective reductant to reduce GO according to a SN^2 nucleophilic reaction. The epoxy groups (Fig. 4a) were ring-opened by the nucleophilic attack of NH_2 groups of histamine and serotonin, followed by the release of H_2O molecules. C=C bonds were thus formed after exiting the intermediate compound. The elimination of carboxylic acid group on GO may occur due to the formation of salt bands (COO^-–NH_3^+) (Fig. 4b). *Nettle* extract can also protect the resulting rGO from free radicals to decrease weathering and corrosion degradation of the substrates beneath rGO coating (Mahmudzadeh et al. 2019).

Diverse plants extraction has recently been used as bio-reductants to produce rGO for different applications. rGO being reduced by *algal* extract (Ahmad et al. 2019) and sugarcane bagasse extract (Li et al. 2018) was applied to remove Cu, Pb and other heavy metals. Reduction by *Spinach* (Suresh et al. 2015a), *Cinnamomum zeylanicum* (Suresh et al. 2015b) and *Syzygium aromaticum* (Suresh et al. 2015c) provided rGO with excellent dye elimination activity toward organic dye and antioxidant activity toward 2,2-diphenyl-1-picrylhydrazyl free radicals. Plant extraction capping was also proven as fine surfactants for rGO to prevent from aggregation and enhanced the biocompatibility as well. rGO being reduced by *Ocimum sanctum* (Shubha et al. 2017) and *Platanus orientalis leaf* extract (Xing et al. 2016) showed less cytotoxic than GO toward Balb 3T3 fibroblasts and cardiac cell lines of Catla, respectively. Extract-reduced rGO via *Allium Cepa* killed 90.5% of *E. coli* in 120 h of incubation (Khanam and Hasan 2019), and 500 µg of grape seed extract-reduced rGO was effective in killing nearly 88% colon cancer cells (Yaragalla et al. 2017).

Table 2 summarized some plant extracts that have been used to reduce GO. Generally, eco-friendly plant extractions are abundant in nature and easily isolated after reduction. More importantly, the reduction reaction could be performed

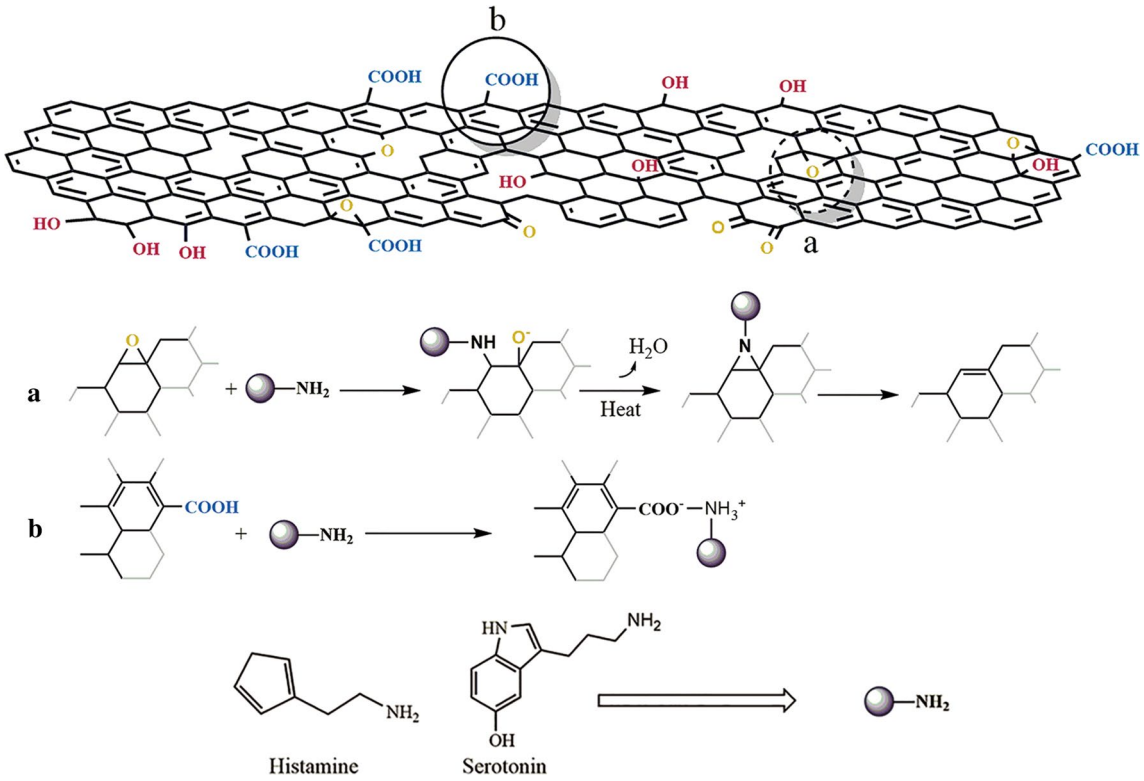

Fig. 4 Mechanism of the reduction process of histamine and serotonin by a nucleophilic reaction of epoxy groups (**a**) and formation of salt band with carboxylic acid groups (**b**) (Mahmudzadeh et al. 2019)

at room temperature and atmospheric pressure, which are very crucial factors for industrial production. The obtained rGO exhibits good biocompatibility for further biomedical applications. Among those green reductants, L-ascorbic acid was proven to be a potential alternative to toxic yet powerful reductants like hydrazine hydrate (Fernández-Merino et al. 2010).

Irradiation reduction

Photocatalytic reduction of GO was initially proposed by Williams and his coworker, where GO powders were reduced to rGO in TiO_2-ethanol colloidal suspension under UV irradiation (Williams et al. 2008). Epoxy and carboxylate groups of GO were first attached to hydroxyl groups on the photocatalytic reductants such as TiO_2, WO_3 and $LaNiO_3$, and the holes were then scavenged to produce ethoxy radicals, leaving the electrons to accumulate within the photocatalytic particles to reduce oxygen-containing groups (Choobtashani and Akhavan 2013). Photo-oxidation is regarded as another mechanism to reduce GO under UV or sun lights. Through TiO_2-supported photolysis, ethanol was oxidized into acetic acid that eliminated carbonyl and epoxide groups of GO dominantly. The reduction time was only 10–15 min, much faster than the above photocatalysis (Lee et al. 2019). Photocatalytic reduction is a very useful method due to its characteristics of energy saving and high efficiency; however, the irradiation time should be controlled strictly because the photodegradation would decrease the carbon content of rGO (Akhavan et al. 2010). More interestingly, rGO improved the photocatalytic activity of its composites with ZnS (Chen et al. 2019), MoS_2 (Li et al. 2019), Boron (Singh et al. 2018), TiO_2 (Raghavan et al. 2018; Yang et al. 2016), V_2O_5 (Aawani et al. 2019) and NiO (Rahimi et al. 2018) because of efficient transfer and rapid separation of photogenerated electrons and holes at the heterojunction. These rGO-composites were considered as one of the most promising materials for photocatalytic degradation of organic pollutant released from leather, plastic, cosmetic and textile industries (Kim et al. 2014a, b).

Microwave reduction utilizes heat transformed from microwave, a form of electromagnetic radiation with frequencies between 300 MHz and 300 GHz. Free-defect basal plane and π electrons of graphene strongly absorb microwave, resulting in the internal and volumetric heating. However, microwave absorption was negatively related to the amount of oxygen-containing groups, and therefore, it was impossible to reduce GO directly. Graphene/GO co-reaction system was reported to successfully reduce GO into rGO,

Table 2 Bio-reduction reaction of GO using various plant extracts

Plants	Reaction condition	Characteristics	Properties	References
Eucalyptus leaf	80 °C, 8 h	C/O ratio: 3.47 I_D/I_G: 1.10	Removing methyl blue completely in about 60 min	Li et al. (2017) Jin et al. (2018)
Spinach	Room temperature, 0.5 h	2θ: 26° UV absorption peak: 282 nm	Removing methylene blue completely in 40 min and malachite green in 60 min Showing ~ 70% inhibition to DPPH free radical (rGO concentration of 590 µg/ml)	Suresh et al. (2015a)
Algal	95 °C, 24 h	2θ: 20°–30° UV absorption peak: 287–288 nm	Decontaminating Cu and Pb in waste water	Ahmad et al. (2019)
Colocasia esculenta leaf	Reflux or room temperature, 8 h or 5 h	C/O ratio: 7.11	Showing good specific capacitance of 17–21 Fg^{-1} Showing high electrical conductivity of 3032.6–4006.0 Sm^{-1}	Thakur and Karak (2012)
Mesua ferrea Linn. leaf	Reflux or room temperature, 10 h or 8 h	C/O ratio: 6.09		
Citrus sinensis peel	Reflux or room temperature, 10 h or 8 h	C/O ratio: 5.97		
Allium Cepa	Room temperature, 6 h	2θ: 26.56°	*E. coli* lost its viability by 45% in 24 h	Khanam and Hasan (2019)
Nettle leaf	90 °C, 1 h	C/O ratio: 4.81 I_D/I_G: 1.13	Showing ~ 70% inhibition to DPPH free radical (rGO concentration of 20 µg/ml)	Mahmudzadeh et al. (2019)
Ocimum sanctum	100 °C, 10 h	2θ: 25°	Showing ~ 90% inhibition to DPPH free radical (rGO concentration of 10 µg/ml) Showing 29% growth inhibition to Balb 3T3 fibroblast cells	Shubha et al. (2017)
Platanus orientalis	100 °C, 10 h	I_D/I_G: 0.95	Showing less cell toxicity than GO	Xing et al. (2016)
Cinnamomum zeylanicum	Reflux, 0.75 h	2θ: 26° UV absorption peak: 280 nm	Showing 50% inhibition to DPPH free radical (rGO concentration of 2250 µg/ml) Removing methylene blue and malachite green completely in 40 min	Suresh et al. (2015b)
Grape seed	Room temperature, 10 h	I_D/I_G: 0.87	Showing activity against 88% colon cancer cells	Yaragalla et al. (2017)
Green tea	Room temperature, 0.5 h Microwave, 1 min	C/O ratio: 7.92 I_D/I_G: 1.40	Adsorbing malachite green dyes in aqueous solution to nearly 416.7 mg/g	Sykam et al. (2018)
Terminalia chebula seed	90 °C, 24 h	I_D/I_G: 2.63	Increasing rGO dispersity	Maddinedi et al. (2015)
Chrysanthemum	95 °C, 24 h	C/O ratio: 4.96 I_D/I_G: 1.138	Enhancing thermal stability	Hou et al. (2016)
Lycium barbarum	95 °C, 24 h	C/O ratio: 6.50 I_D/I_G: 1.045	Showing high thermal stability	Hou et al. (2017)
Sugarcane bagasse	95 °C, 12 h Ammonia	C/O ratio: 4.27 I_D/I_G: 1.16	Adsorbing Cd (II) in aqueous solution to nearly 24.47 mg/g	Li et al. (2018)

Table 2 (continued)

Plants	Reaction condition	Characteristics	Properties	References
Syzygium aromaticum	100 °C, 0.5 h	2θ: 23.9°	Removing methylene blue and malachite green completely within 20 min; Showing 50% inhibition to DPPH free radical (rGO concentration of 1337 µg/ml)	Suresh et al. (2015c)

because heat released from graphene would superheat the adjacent GO and contribute to local reduction under the microwave irradiation. Once GO deoxygenated to a certain degree, it would act as another heat absorbent to accelerate the process (Menendez et al. 2010; Hu et al. 2012). Considering that residue graphene can be hardly removed from rGO, Tang et al. (2019) designed a layer of mildly reduced GO membrane as a microwave absorbent and obtained rGO with C/O ratio up to 17.84 under argon at 2000 W for only 30 s.

Laser irradiation causes local heat to trigger the deoxidation reaction of GO, and the reduction degree can be controlled by the irradiation parameters including wavelength, power density, scanning speed, beam energy profile or focusing and processing conditions (Zhang et al. 2014a, b; Yang et al. 2018a, b). During the reduction process, the local temperature raised to approximately 500 °C via a 663-nm continuous wave diode laser (Zhou et al. 2010) and was even higher up to 1400 °C under the irradiation of 1064-nm picosecond laser (Trusovas et al. 2013). Laser irradiation produced rGO in a tunable reduction degree, though the elimination of water molecules and oxygen-containing groups by evaporation might cause the surface defects. Different from most laser sources that required complex and high-cost instrument, continuous wave CO_2 laser is an inexpensive technology, showing potential application for mass production of rGO. CO_2 laser at the wavelength of 10.6 µm has a far more penetration depth than any kind of laser mentioned above; therefore, the pyrolysis can eliminate extremely fast the oxygen-containing groups of GO to produce rGO with different size of pores randomly arranged in the cross-sectional surface. rGO showed the equivalent series resistance and interface resistance, respectively, of 0.52 Ω and 0.93 Ω and the specific capacitance of 35 F g^{-1}, illustrating excellent electrochemical performances for potential symmetric supercapacitor application (Bhattacharjya et al. 2018).

Plasma, one of the fundamental states of matter, can be artificially generated by heat, high-pressure discharge or strong electromagnetic field. Via activation by electron beam, gas molecules generate various radicals and ions that react with oxygen-containing groups to restore the defects and/or dope atoms on the carbon basal plane (Yu et al. 2013). Several plasma have already been employed in the reduction of GO (Table 3); however, oxygen plasma can even introduce oxygen-containing groups on rGO surface reversely (Kondratowicz et al. 2018). Hydrogen plasma produced atomic hydrogen to react and remove oxygen groups from GO films at low temperatures (< 150 °C) (Lee et al. 2012), much lower temperature than the thermal reduction. Hydrogen plasma removed as much oxygen as chemical reduction by $NaBH_4$, but it was simpler, faster and cleaner, and the remaining oxygen formed labile groups (Alotaibi et al. 2018). However, hydrogen plasma treatment might lead to high defective rGO and was often limited by the etching effect of active hydrogen atoms (Li et al. 2015). A CH_4 remote plasma for GO pre-treated via chemical vapor deposition was reported to reduce the defect greatly. rGO became thinner and smoother due to eliminating sp^3 carbon domains as the treatment time increased (Cheng et al. 2012). Under the flux of Ar/CH_4 plasma using Ar as a promoter, CH_4 molecules were dissociated into CH_x ($X < 4$) radicals and active H ions through the collision with high-energy electrons, which can react with oxygen-containing groups of GO. The remaining CH_x radicals and amorphous carbon species were then deposited on the carbon lattice (Yang et al. 2018a, b). Ar/CH_4 mixture plasma provided a potential method to produce thin film because of low impact on GO surface, tunable oxygen content and growth of sp^2 cluster (Baraket et al. 2010). NH_3 plasma was not only able to reduce GO, but also to introduce nitrogen element on the carbon lattice to alter the electrical conductivity and transmittance greatly. The conductivity of rGO films was reported to increase from 100 to 1666 S/m with plasma treatment time (Kim et al. 2013; Kim and Choi 2014). Plasma exfoliation under several gas (O_2, N_2, CH_4) can prepare graphene from GO at room temperature efficiently and environment friendly. It was believed that oxygen was produced during the treatment due to the breaking of C–O bond and generating oxygen molecules under the ion bombardment. GO-CH_4 based electrodes showed excellent power and energy density (597.2 W kg^{-1} at 14.93 Wh kg^{-1}), demonstrating their potential applications as supercapacitors (Wang et al. 2015). Nevertheless, most plasma treatment required high sophisticated equipment, specific environment and pumping system and can use only small size of samples in batch mode that limited their scalability and application for large samples and mass production of films and devices.

Table 3 Properties and reaction condition of rGO via different plasma reduction

Method	Reaction condition	Characteristics and properties	References
H_2 plasma	60 W, 30 min	Resistance: 1.62 MΩ/sq I_D/I_G ratio: 0.93	Li et al. (2015)
H_2 plasma	500 W/700 W, 1–10 min	C/O ratio: 2.54 (500 w, 1 min); 3.02 (500 w, 5 min) 2.70 (500 w, 10 min); 3.09 (700 w, 5 min) I_D/I_G ratio: 0.87 (700 w, 5 min)	Abdelkader-Fernández et al. (2019)
H_2/Ar plasma	150 °C, 30 min	C/O ratio: 6.95 Sheet resistance: 4.77×10^4 Ω/sq	Lee et al. (2012)
CH_4 plasma	0.20 Torr, 100 W	Resistance at the Dirac point: 9.0 kΩ/sq I_D/I_G ratio: 0.53	Cheng et al. (2012)
CH_4/Ar plasma	100 W, 10 min	Resistance: 320.6 Ω/sq C/O ratio: 11.6 I_D/I_G ratio: 1.11	Yang et al. (2018a, 2018b)
CH_4/Ar plasma	90 mTorr, 30 s	I_D/I_G ratio: 0.7–1	Baraket et al. (2010)
NH_3 plasma	200 W, 3 min	Resistance: 67.5 kΩ/sq I_D/I_G ratio: 0.98 Electrical conductivity of 7.4 S/cm for 6% N-doped rGO	Kim et al. (2013)
NH_3 plasma	10 W, 100 mTorr, 30 min	N/C ratio: 9% O/C ratio: 25% Transmittance at 600 nm decreasing from 85.9% to 45% Via NH_3 plasma treatment for 30 min	Kim et al. (2014a, 2014b)
O_2, N_2, CH_4 plasma	70 W	Energy density (Wh kg^{-1}): 14.93 (GO-CH_4); 6.11 (GO-N_2); 8.96 (GO-O_2) Power density (W kg^{-1}): 597.2 (GO-CH_4); 244.4 (GO-N_2); 358.4 (GO-O_2)	Wang et al. (2015)

More interestingly, plasma or laser irradiation has also demonstrated its capability in patterning rGO. Atmospheric plasma with high electron densities ($> 10^{13}$ cm^{-3}) and energetic electrons (> 20 eV) produced reactive gas species and radicals to ionize and remove the oxygen groups on GO. A short reduction time of 60 s at room temperature provided rGO films with a resistance of 160 Ω/sq without damaging their structure, which was impossible to achieve by conventional wet chemical and thermal reduction process. While combined with a *x*–*y* scanning plasma software, rGO films were also allowed to introduce various patterns on the surface of glass, plastic or textile with various shapes, showing patterning capability with low defects and high conductivity (Alotaibi et al. 2018). rGO lines being doped via a femtosecond laser ($\lambda = 795$ nm) exhibited 5 order-of-magnitude decrease in resistivity compared to a non-irradiated sample (Kang et al. 2018). Periodic patterns of rGO being obtained by a femtosecond laser at higher fluences than the reduction of GO can modify the surface chemical composition, and the ripples appeared either after or simultaneously with the reduction reaction. However, the authors did not entirely interpret the formation of laser-induced periodic patterns on rGO (Kasischke et al. 2018). A single technique to simultaneously reduce and periodically pattern GO can accelerate and simplify the production of graphene nanostructures, which will be prone to realize the complex integration of graphene-based devices.

Generally, irradiation reduction is superior to other methods in the aspect of extremely short reaction period and effectively repairing defects in the carbon plane, although relatively expensive equipment and special condition are usually needed.

Electrochemical reduction

Electrochemical reduction derived from the electron being transferred from anode to GO in a standard electrochemical cell, where reaction parameters including the applied voltage, electrical current, electrolyte solution and reduction time played important roles in GO reduction (Toh et al. 2014; Alanyalioglu et al. 2012). Theoretically, the increase in reaction time led to a large degree of GO reduction, and overpotential was often required to achieve more complete rGO (Kauppila et al. 2013). Since organic solvents had broader potential windows than aqueous solutions, more negative potentials would be applied to obtain rGO with a very high C/O ratio on the surface of Si substrate (Marrani et al. 2018). Acidic or near neutral electrochemical medium was also reported to be suitable for chemical reduction of GO (Dreyer et al. 2010).

The electrochemical reduction can be classified into one-step and two-step approaches. In the one-step electrochemical reduction, the negatively charged GO in electrolytic

buffer was attracted by anode, and rGO thin film was eventually produced on the electrode surface due to the different solubility between GO and rGO (Liu et al. 2011). In the two-step electrochemical reduction, GO thin film was pre-assembled onto anode and then subjected to reduction using a standard three-electrode system in the presence of a buffer or supporting electrolyte to produce rGO films. Compared with the one-step electrochemical reduction, the latter can obtain desirable size, shape and thickness of rGO by controlling the deposition on electrode, which relied on the deposition techniques and parameters used (Eda and Chhowalla 2010; Paredes et al. 2008).

The oxygen-containing groups of GO were reported to be eliminated at different potentials during the electrochemical reduction. For example, the carbonyl groups were reduced at − 1.3 V, while hydroxy and epoxyl groups at − 1.5 V (Guo et al. 2009). More interestingly, the amount of hydroxyl groups reduced slightly or even increased during the elimination of epoxyl groups, perhaps due to the fact that the hydroxy bonds remained as carboxylate and epoxyl groups were reduced (Marrani et al. 2018; García-Argumánez et al. 2019). As illustrated in Fig. 5, carboxylate groups were eliminated and the resulting α-rGO was further reduced to β-rGO (Fig. 5a), where methyl groups were formed instead of the remanent oxygen-containing groups and a π-conjugated lattice was formed either (Kmen et al. 2017). On the other hand, carbonyl groups were converted into hydroxyl groups at the edge of rGO through one-electron approach (Fig. 5b), and epoxyl groups were reported to convert into C=C bonds through two-electron mechanism (Fig. 5c) (Marrani et al. 2019). In the electrochemical reducing process, the transfer of electrons to rGO was carried out by the proton transfer involving the solvent. Electrochemical reduction is extremely useful when directly fabricating symmetric rGO-based supercapacitor, biosensor, electrocatalysis without further treatment. It is also regarded as an eco-friendly, rapid method to produce rGO.

Microbial reduction

Microorganisms that metabolize with energy release and electron transfer are able to utilize some molecules to displace the deficiency of the corresponding essential

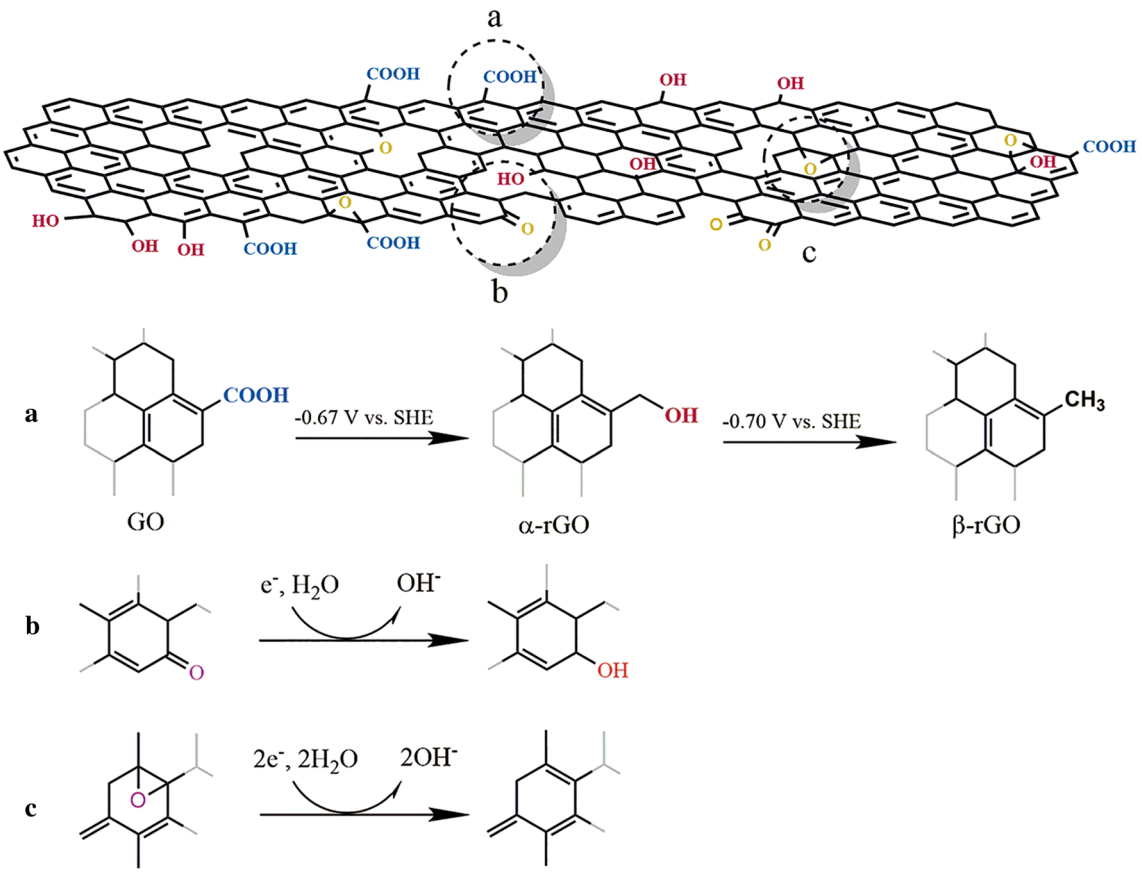

Fig. 5 Mechanism of GO reduction via different process: **a** two-step reaction of reducing carboxylic acid groups (Kmen et al. 2017); **b** one-step reaction of reducing carbonyl groups via one-electron approach; **c** one-step reaction of reducing epoxy groups via two-electron approach (Marrani et al. 2019)

substance such as respiratory substrate. The possibility for GO to participate in the metabolism has inspired scientists to synthesis rGO by incubating with microorganisms. *Shewanella* species was proven as GO-reduced bacterial via respiration in an anaerobic or aerobic condition (Salas et al. 2010). Interior electrons being produced by the bacterial respiration were transferred to GO and ultimately led to the reduction. This process was mediated by outer membrane c-type cytochromes (Mtr/Omc) and self-secreted electron mediators, in which MtrA, MtrB and CymA comprised the transfer pathway, while MtrF was dispensable (Jiao et al. 2011). *E. coli* was also reported to reduce GO in mixed-acid fermentation under an anaerobic condition through electron transference in metabolic activity (Jiao et al. 2011). Interestingly, the proliferation of *E. coil* on rGO surface decreased significantly while compared with GO, in consistent with "self limiting" or "self killing" effect that the cytotoxicity of rGO was higher than GO (Zou et al. 2016; Jiao et al. 2011).

Bio-enzyme being produced by bacteria could remove the oxygen-containing groups directly or indirectly. Baker's yeast containing NAPDH was utilized to reduce the epoxy ketones of GO, forming C-NH on the surface. Nitrogenase from *Azotobacter chroococcum* was an effective bio-enzyme when bound on femo-cofactor, where the oxygen-containing groups received electrons/protons and were eventually removed by dehydration reactions. However, C/O ratios of rGO reduced by baker's Yeast and *Azotobacter chroococcum* were, respectively, 5.9 and 4.18, much lower than the reduction process by $NaBH_4$ (15.1) and hydrazine (10.4) (Khanra et al. 2012; Chen et al. 2017). Other bacteria, such as *Bacillus sibtilus* (Zhang et al. 2013a, b), *Extremophiles bacteria* (Raveendran et al. 2013) and *Gluconacetobacter xylinus* (Nandgaonkar et al. 2014), have also been used to reduce GO. Microbial reduction is a potential method for large-scale rGO synthesis in an eco-friendly, cost effective and simple way, though it needs long reduction time and careful culture procedure.

Conclusions and major challenges

The reduction routes of GO and the possible mechanism were reviewed with an aim at promoting the application of graphene and its derivatives (Table 4), though no optimal method was settled especially for large-scale industrial production. Various oxygen-containing groups on GO sheets were removed via different routes chemically or physically, and these methods showed confining high activity toward certain oxygen functional groups. Because precise oxidation of GO via a reliable technique was still questionable, it was very difficult to control the reduction degree precisely and repeatedly. Therefore, multistep reduction strategies might allow us to eliminate specific functional groups more precisely. In addition, method combining reduction with pattern of rGO was a fast and simple direct treatment to produce conductive rGO films and print different patterns on GO device under environmentally friendly conditions without damaging the underlying substrate. It still needs a deeper understanding of graphene structure and fabrication technology for scalable production of these rGO-based devices.

Table 4 Four main reduction methods

Method	Representative reaction condition	Features
Reduction via reductant	Chemical reductant: hydrazine, sodium borohydride	Performing at relatively low temperature Conflict of reduction effectiveness and compatibility of reductant
	Solvothermal reductant: *N*,*N*-dimethylformamide, vinylpyrrolidone	Producing a stable dispersion of rGO without any extra chemical reductant Requiring special equipment and rigorous condition
	Bio-reductants: L-ascorbic, L-cysteine, plant extraction	Being abundant in nature and easily isolated after reduction Performing at relatively low temperature Presenting good biocompatibility and dispersity in water Exhibiting relatively weak reduction efficiency
Irradiation reduction	Photocatalytic reduction: UV, visible light; solar light Plasma reduction: H_2; CH_4; NH_3 Microwave	Short reaction period Effectively repairing defects in the carbon plane Requiring special equipment and rigorous condition
Electrochemical reduction	Working electrode: Si, glassy carbon, SnO_2 glass Reference electrode: Ag/AgCl, SCE Counter electrode: platinum wire Supporting electrolyte: PBS, KCl, KOH	Directly fabricating rGO-based supercapacitor, biosensor, electrocatalysis without further treatment Eco-friendly and rapid Deposition of GO onto electrode limiting the large-scale production
Microbial reduction	*Shewanella*, *E. coli*, yeast, *Azotobacter chroococcum*	Cost effective and simple Requiring long time and careful culture procedure

Acknowledgements This study was financially supported by the National Natural Science Foundation of China (51572110, 31470934), the Guangdong Natural Science Foundation of China (2016A030313085), the Guangdong Science and Technology Program Key project of China (2014B010105007) and the Guangdong Science and Technology Project of China (2015A020212025).

Compliance with ethical standards

Conflict of interest The authors declare that they have no conflict of interest.

References

Aawani E, Memarian N, Dizaji HR (2019) Synthesis and characterization of reduced graphene oxide-V_2O_5 nanocomposite for enhanced photocatalytic activity under different types of irradiation. J Phys Chem Solids 125:8–15. https://doi.org/10.1016/j.jpcs.2018.09.028

Abdelkader-Fernández VK, Melguizo M, Domingo-García M, López-Garzón FJ, Pérez-Mendoza M (2019) Hydrogen cold plasma for the effective reduction of graphene oxide. Appl Surf Sci 464:673–681. https://doi.org/10.1016/j.apsusc.2018.09.121

Ahmad S, Ahmad A, Khan S, Ahmad S, Khan I, Zada S, Fu P (2019) Algal extracts based biogenic synthesis of reduced graphene oxides (rGO) with enhanced heavy metals adsorption capability. J Ind Eng Chem 72:117–124. https://doi.org/10.1016/j.jiec.2018.12.009

Akhavan O, Abdolahad M, Esfandiar A, Mohatashamifar M (2010) Photodegradation of graphene oxide sheets by TiO_2 nanoparticles after a photocatalytic reduction. J Phys Chem C 114:12955–12959. https://doi.org/10.1021/jp103472c

Akhavan O, Ghaderi E, Aghayee S, Fereydooni Y, Talebi A (2012) The use of a glucose-reduced graphene oxide suspension for photothermal cancer therapy. J Mater Chem 22:13773–13781. https://doi.org/10.1039/C2JM31396K

Alanyalioglu M, Seruga JJ, Oro-Sole J, Casan-Pastor N (2012) The synthesis of graphene sheets with controlled thickness and order using surfactant-assisted electrochemical processes. Carbon 50:142–152. https://doi.org/10.1016/j.carbon.2011.07.064

Alotaibi F, Tung TT, Nine MJ, Kabiri S, Moussa M, Tran DNH, Losic D (2018) Scanning atmospheric plasma for ultrafast reduction of graphene oxide and fabrication of highly conductive graphene films and patterns. Carbon 127:113–121. https://doi.org/10.1016/j.carbon.2017.10.075

Amiri A, Naraghi M, Ahmadi G, Soleymaniha M, Shanbedi M (2018) A review on liquid-phase exfoliation for scalable production of pure graphene, wrinkled, crumpled and functionalized graphene and challenges. Flat Chem 8:40–71. https://doi.org/10.1016/j.flatc.2018.03.004

Balasubramaniam M, Balakumar S (2016) Tri-solvent mediated probing of ultrasonic energy towards exfoliation of graphene nanosheets for supercapacitor application. Mater Lett 182:63–67. https://doi.org/10.1016/j.matlet.2016.06.088

Balasubramaniam M, Balakumar S (2017a) On the development of hierarchical nanostructures of graphene-zinc antimonate as inexpensive electrode materials for supercapacitors. Electrochim Acta 253:178–189. https://doi.org/10.1016/j.electacta.2017.09.006

Balasubramaniam M, Balakumar S (2017b) Concept of collective Nernstian-Capacitive mechanism in graphene nanosheets for electrochemical energy storage. AIP Conf Proc 1832:050091. https://doi.org/10.1063/1.4980324

Baraket M, Walton SG, Wei Z, Lock EH, Robinson JT, Sheehan P (2010) Reduction of graphene oxide by electron beam generated plasmas produced in methane/argon mixtures. Carbon 48:3382–3390. https://doi.org/10.1016/j.carbon.2010.05.031

Becerril HA, Mao J, Liu Z, Stoltenberg RM, Bao Z, Chen Y (2008) Evaluation of solution-processed reduced graphene oxide films as transparent conductors. ACS Nano 2:463–470. https://doi.org/10.1021/nn700375n

Bhattacharjya D, Kim CH, Kima JH, Youd IK, In JB, Lee SM (2018) Fast and controllable reduction of graphene oxide by low-cost CO_2 laser for supercapacitor application. Appl Surf Sci 462:353–361. https://doi.org/10.1016/j.apsusc.2018.08.089

Botas C, Álvarez P, Blanco P, Granda M, Blanco C, Santamaría R, Romasanta L, Verdejo R, López-Manchado M, Menéndez R (2013) Graphene materials with different structures prepared from the same graphite by the Hummers and Brodie methods. Carbon 65:156–164. https://doi.org/10.1016/j.carbon.2013.08.009

Brodie B (1859) On the atomic weight of graphite. Philos Trans 149:249–259. https://doi.org/10.1098/rstl.1859.0013

Chen D, Li L, Guo L (2011) An environment-friendly preparation of reduced graphene oxide nanosheets via amino acid. Nanotechnology 22:325601. https://doi.org/10.1088/0957-4484/22/32/325601

Chen H, Song Z, Zhao X, Li X, Lin H (2013) Reduction of free-standing graphene oxide papers by a hydrothermal process at the solid/gas interface. RSC Adv 3:2971–2978. https://doi.org/10.1039/C2RA21576D

Chen Y, Niu Y, Tian T, Zhang J, Wang Y, Li Y, Qin L (2017) Microbial reduction of graphene oxide by Azotobacter chroococcum. Chem Phys Lett 677:143–147. https://doi.org/10.1016/j.cplett.2017.04.002

Chen X, Li H, Chen M, Li W, Yuan Z, Snyders R (2019) Visible-light-driven photocatalytic activities of monodisperse ZnS-coated reduced graphene oxide nanocomposites. Mater Chem Phys 227:368–374. https://doi.org/10.1016/j.matchemphys.2019.01.055

Cheng M, Yang R, Zhang L, Shi Z, Yang W, Wang D, Xie G, Shi D, Zhang G (2012) Restoration of graphene from graphene oxide by defect repair. Carbon 50:2581–2587. https://doi.org/10.1016/j.carbon.2012.02.016

Chi H, Murali K, Li T, Thomas S (2019) Recent advances in graphene based photoresponsive materials. Prog Nat Sci Mater . https://doi.org/10.1016/j.pnsc.2019.11.002

Choobtashani M, Akhavan O (2013) Visible light-induced photocatalytic reduction of graphene oxide by tungsten oxide thin films. Appl Surf Sci 276:628–634. https://doi.org/10.1016/j.apsusc.2013.03.144

Dreyer DR, Park S, Bielawski CW, Ruoff RS (2010) The chemistry of graphene oxide. Chem Soc Rev 39:228–240. https://doi.org/10.1039/B917103G

Dubin S, Gilje S, Wang K, Tung VC, Cha K, Hall AS, Farrar J, Varshneya R, Yang Y, Kaner RB (2010) A one-step, solvothermal reduction method for producing reduced graphene oxide dispersions in organic solvents. ACS Nano 4:3845–3852. https://doi.org/10.1021/nn100511a

Eda G, Chhowalla M (2010) Chemically derived graphene oxide: towards large-area thin-film electronics and optoelectronics. Adv Mater 22:2392–2415. https://doi.org/10.1002/adma.200903689

Elgengehi SM, El-Taher S, Ibrahim MAA, Desmarais JK, El-Kelany KE (2020) Graphene and graphene oxide as adsorbents for cadmium and lead heavy metals: a theoretical investigation. Appl Surf Sci 507:145038. https://doi.org/10.1016/j.apsusc.2019.145038

Fernández-Merino MJ, Guardia L, Paredes JI, Villar-Rodil S, Solís-Fernández P, Martínez-Alonso A, Tascón JMD (2010) Vitamin C is an ideal substitute for hydrazine in the reduction of graphene

oxide suspensions. J Phys Chem C 114:6426–6432. https://doi.org/10.1021/jp100603h
Galeotti F, Barile E, Curir P, Dolci M, Lanzotti V (2008) Flavonoids from carnation (*Dianthus caryophyllus*) and their antifungal activity. Phytochem Lett 1:4–48. https://doi.org/10.1016/j.phytol.2007.10.001
Gao J, Liu F, Liu Y, Ma N, Wang Z, Zhang X (2010) Environment-friendly method to produce graphene that employs vitamin C and amino acid. Chem Mater 22:2213–2218. https://doi.org/10.1021/cm902635j
García-Argumánez A, Llorente I, Caballero-Calero O, González Z, Menéndez R, Escudero ML, García-Alonso MC (2019) Electrochemical reduction of graphene oxide on biomedical grade CoCr alloy. Appl Surf Sci 465:1028–1036. https://doi.org/10.1016/j.apsusc.2018.09.188
Guo HL, Wang XF, Qian QY, Wang FB, Xia XH (2009) A green approach to the synthesis of graphene nanosheets. ACS Nano 3:2653–2659. https://doi.org/10.1021/nn900227d
Guo J, Ren L, Wang R, Zhang C, Yang Y, Liu T (2011) Water dispersible graphene noncovalently functionalized with tryptophan and its poly(vinyl alcohol) nanocomposite. Compos Part B-Eng 42:2130–2135. https://doi.org/10.1016/j.compositesb.2011.05.008
Hanifah MFR, Jaafar J, Aziz M, Ismail AF, Othman MHD, Rahman MA, Norddin MNAN, Yusof N, Salleh WNW (2015) Efficient reduction of graphene oxide nanosheets using $Na_2C_2O_4$ as a reducing agent. Funct Mater Lett 2:1550026. https://doi.org/10.1142/S1793604715500265
Hou D, Liu Q, Cheng H, Li K, Wang D, Zhang H (2016) Chrysanthemum extract assisted green reduction of graphene oxide. Mater Chem Phys 183:76–82. https://doi.org/10.1016/j.matchemphys.2016.08.004
Hou D, Liu Q, Cheng H, Zhang H, Wang S (2017) Green reduction of graphene oxide via *Lycium barbarum* extract. J Solid State Chem 246:351–356. https://doi.org/10.1016/j.jssc.2016.12.008
Hou D, Liu Q, Wang X, Quan Y, Qiao Z, Yu L, Ding S (2018) Facile synthesis of graphene via reduction of graphene oxide by artemisinin in ethanol. J Materiomics 4:256–265. https://doi.org/10.1016/j.jmat.2018.01.002
Hu H, Zhao Z, Zhou Q, Gogotsi Y, Qiu J (2012) The role of microwave absorption on formation of graphene from graphite oxide. Carbon 50:3267–3273. https://doi.org/10.1016/j.carbon.2011.12.005
Huang X, Yin Z, Wu S, Qi X, He Q, Zhang Q, Yan Q, Boey F, Zhang H (2011) Graphene-based materials: synthesis, characterization, properties, and applications. Small 7:1876–1902. https://doi.org/10.1002/smll.201002009
Hummers WS, Offeman RE (1958) Preparation of graphitic oxide. J Am Chem Soc 80:1339. https://doi.org/10.1021/ja01539a017
Jiao Y, Qian F, Li Y, Wang G, Saltikov CW, Gralnick JA (2011) Deciphering the electron transport pathway for graphene oxide reduction by *Shewanella oneidensis* MR-1. J Bacteriol 193:3662–3665. https://doi.org/10.1128/JB.00201-11
Jin X, Li N, Weng X, Li C, Chen Z (2018) Green reduction of graphene oxide using eucalyptus leaf extract and its application to remove dye. Chemosphere 208:417–424. https://doi.org/10.1016/j.chemosphere.2018.05.199
Kamat PV (2009) Graphene-based nanoarchitectures: anchoring semiconductor and metal nanoparticles on a two-dimensional carbon support. J Phys Chem Lett 1:520–527. https://doi.org/10.1021/jz900265j
Kang SY, Evans CC, Shukla S, Reshef O, Mazur E (2018) Patterning and reduction of graphene oxide using femtosecond-laser irradiation. Opt Laser Technol 103:340–345. https://doi.org/10.1016/j.optlastec.2018.01.059
Kasischke M, Maragkaki S, Volz S, Ostendorf A, Gurevich EL (2018) Simultaneous nanopatterning and reduction of graphene oxide by femtosecond laser pulses. Appl Surf Sci 445:197–203. https://doi.org/10.1016/j.apsusc.2018.03.086
Kauppila J, Kunnas P, Damlin P, Viinikanoja A, Kvarnström C (2013) Electrochemical reduction of graphene oxide films in aqueous and organic solutions. Electrochim Acta 89:84–88. https://doi.org/10.1016/j.electacta.2012.10.153
Kavimani V, Prakash KS, Rajesh R, Rammasamy D, Selvaraj NB, Yang T, Prabakaran B, Jothi S (2017) Electrodeposition of r-GO/SiC nano-composites on magnesium and its corrosion behavior in aqueous electrolyte. Appl Surf Sci 424:63–71. https://doi.org/10.1016/j.apsusc.2017.02.082
Khanam PN, Hasan A (2019) Biosynthesis and characterization of graphene by using non-toxic reducing agent from *Allium cepa* extract: anti-bacterial properties. Int J Biol Macromol 126:151–158. https://doi.org/10.1016/j.ijbiomac.2018.12.213
Khanra P, Kuila T, Kim NH, Bae SH, Yu D, Lee JH (2012) Simultaneous bio-functionalization and reduction of graphene oxide by Baker's yeast. Chem Eng J 183:526–533. https://doi.org/10.1016/j.cej.2011.12.075
Kim SP, Choi HC (2014) Photocatalytic degradation of methylene blue in presence of graphene oxide/TiO_2 nanocomposites. Bull Korean Chem Soc 35:2660–2664. https://doi.org/10.5012/bkcs.2014.35.9.2660
Kim MJ, Jeong Y, Sohn SH, Lee SY, Kim YJ, Lee K, Kahng YH, Jang J (2013) Fast and low-temperature reduction of graphene oxide films using ammonia plasma. AIP Adv 3:012117. https://doi.org/10.1063/1.4789545
Kim SJ, Choi K, Park SJ (2014a) A facile approach to prepare graphene via solvothermal reduction of graphite oxide. Mater Res Bull 55:48–52. https://doi.org/10.1016/j.materresbull.2014.04.016
Kim HT, Kim C, Park C (2014b) Reduction and nitridation of graphene oxide (GO) films at room temperature using inductively coupled NH_3 plasma. Vacuum 108:35–38. https://doi.org/10.1016/j.vacuum.2014.05.018
Kim SJ, Choi K, Park SJ (2016) Solvothermal reduction of graphene oxide in dimethylformamide. Solid State Sci 61:40–43. https://doi.org/10.1016/j.solidstatesciences.2016.07.013
Kmen MP, Casas IF, Naghilou A, Trettenhahn G, Kautek W (2017) A multivariate curve resolution evaluation of an in situ ATR-FTIR spectroscopy investigation of the electrochemical reduction of graphene oxide. Electrochim Acta 255:160–167. https://doi.org/10.1016/j.electacta.2017.09.124
Kondratowicz I, Nadolska M, Sahin S, Lapinski M, Przesniak WM, Sawczak M, Yu EH, Sadowski W, Zelechowska K (2018) Tailoring properties of reduced graphene oxide by oxygen plasma treatment. Appl Surf Sci 440:651–659. https://doi.org/10.1016/j.apsusc.2018.01.168
Krishna R, Fernandes DM, Venkataramana E, Dias C, Ventura J, Freire C, Titus E (2015) Improved reduction of graphene oxide. Mater Today Proc 2:423–430. https://doi.org/10.1016/j.matpr.2015.04.049
Lee SW, Mattevi C, Chhowalla M, Sankaran RM (2012) Plasma-assisted reduction of graphene oxide at low temperature and atmospheric pressure for flexible conductor applications. Phys Chem Lett 3:772–777. https://doi.org/10.1021/jz300080p
Lee G, Jung DW, Lee W, Nah S, Ji S, Hwang JY, Lee SS, Park S, Chae SS, Lee JO (2019) Solution-processable method for producing high-quality reduced graphene oxide displaying 'self-catalytic healing'. Carbon 141:774–778. https://doi.org/10.1016/j.carbon.2018.09.038
Li T, Patel T, Banerjee I, Pearce-Hill R, Gallop J, Hao L, Asim K (2015) Plasma treated graphene oxide films: structural and electrical studies. Mater Electron 26:4810–4815. https://doi.org/10.1007/s10854-015-3122-0

Li C, Zhuang Z, Jin X, Chen Z (2017) A facile and green preparation of reduced graphene oxide using *Eucalyptus* leaf extract. Appl Surf Sci 422:469–474. https://doi.org/10.1016/j.apsusc.2017.06.032

Li B, Jin X, Lin J, Chen Z (2018) Green reduction of graphene oxide by sugarcane bagasse extract and its application for the removal of cadmium in aqueous solution. J Clean Prod 189:128–134. https://doi.org/10.1016/j.jclepro.2018.04.018

Li H, Li W, Yang H, Lia W, Yuan Z, Chen M, Bittencourt C, Snyders R (2019) Photocatalytic properties of MoS_2 nanoflakes vertically assembled on reduced graphene oxide. Thin Solid Films 672:176–181. https://doi.org/10.1016/j.tsf.2018.12.020

Lin T, Chen I, Liu F, Yang C, Bi H, Xu F, Huang F (2015) Nitrogen-doped mesoporous carbon of extraordinary capacitance for electrochemical energy storage. Science 350:1508–1513. https://doi.org/10.1126/science.aab3798

Liu C, Wang K, Luo S, Tang Y, Chen L (2011) Direct electrodeposition of graphene enabling the one-step synthesis of graphene-metal nanocomposite films. Small 7:1203–1206. https://doi.org/10.1002/smll.201002340

Maddinedi SB, Mandal BK, Vankayala R (2015) Bioinspired reduced graphene oxide nanosheets using *Terminalia chebula* seeds extract. Spectrochim Acta A 145:117–124. https://doi.org/10.1016/j.saa.2015.02.037

Mahmudzadeh M, Yari H, Ramezanzadeh B, Mahdavian M (2019) Highly potent radical scavenging-anti-oxidant activity of biologically reduced graphene oxide using *Nettle* extract as a green bio-genic amines-based reductants source instead of hazardous hydrazine hydrate. J Hazard Mater 371:609–624. https://doi.org/10.1016/j.jhazmat.2019.03.046

Marcano DC, Kosynkin DV, Berlin JM, Sinitskii A, Sun ZZ, Slesarev A, Alemany LB, Lu W, Tour JM (2010) Improved synthesis of graphene oxide. ACS Nano 4:4806–4814. https://doi.org/10.1021/nn1006368

Marrani AG, Coico AC, Giacco D, Zanoni R, Scaramuzzo FA, Schrebler R, Dini D, Bonomo M, Dalchiele EA (2018) Integration of graphene onto silicon through electrochemical reduction of graphene oxide layers in non-aqueous medium. Appl Surf Sci 445:404–414. https://doi.org/10.1016/j.apsusc.2018.03.147

Marrani AG, Motta A, Schrebler R, Zanoni R, Dalchiele EA (2019) Insights from experiment and theory into the electrochemical reduction mechanism of graphene oxide. Electrochim Acta 304:231–238. https://doi.org/10.1016/j.electacta.2019.02.108

Menendez JA, Arenillas A, Fidalgo B, Fernandez Y, Zubizarreta L, Calvo EG (2010) Microwave heating processes involving carbon materials. Fuel Process Technol 91:1–8. https://doi.org/10.1016/j.fuproc.2009.08.021

Muzyka R, Kwoka M, Smędowski L, Díez N, Gryglewicz G (2017) Oxidation of graphite by different modified Hummers methods. New Carbon Mater 32:15–20. https://doi.org/10.1016/S1872-5805(17)60102-1

Nandgaonkar AG, Wang Q, Fu K, Wendy E, Krause WE, Wei Q, Gorga R, Lucia ALA (2014) A one-pot biosynthesis of reduced graphene oxide (RGO)/bacterial cellulose (BC) nanocomposites. Green Chem 16:3195–3201. https://doi.org/10.1039/C4GC00264D

Navik R, Gai Y, Wang W, Zhao Y (2018) Curcumin-assisted ultrasound exfoliation of graphite to graphene in ethanol. Ultrason Sonochem 48:96–102. https://doi.org/10.1016/j.ultsonch.2018.05.010

Nayak TR, Andersen H, Makam VS, Khaw C, Bae S, Xu X, Ee PR, Ahn JH, Hong BH, Pastorin G, Ozyilmaz B (2011) Graphene for controlled and accelerated osteogenic differentiation of human mesenchymal stem cells. ACS Nano 5:4670–4678. https://doi.org/10.1021/nn200500h

Ng YH, Iwase A, Kudo A, Amal R (2010) Reducing graphene oxide on a visible-light $BiVO_4$ photocatalyst for an enhanced photoelectrochemical water splitting. J Phys Chem Lett 17:2607–2612. https://doi.org/10.1021/jz100978u

Novoselov KS, Geim AK, Morozov SV, Jiang D, Zhang Y, Dubonos SV, Grigorieva IV, Firsov AA (2004) Electric field effect in atomically thin carbon films. Science 306:666–669. https://doi.org/10.1126/science.1102896

Paredes JI, Villar-Rodil S, Martinez-Alonso A, Tascon JMD (2008) Graphene oxide dispersions in organic solvents. Langmuir 24:10560–10564. https://doi.org/10.1021/la801744a

Park G, Park SK, Han J, Ko TY, Seungjun L, Oh J, Ryu S, Park HO, Park S (2014) Finely tuning oxygen functional groups of graphene materials and optimizing oxygen levels for capacitors. RSC Adv 4:36377–36384. https://doi.org/10.1039/C4RA02873B

Pei S, Cheng H (2012) The reduction of graphene oxide. Carbon 50:3210–3228. https://doi.org/10.1016/j.carbon.2011.11.010

Pei S, Zhao J, Du J, Ren W, Cheng HM (2010) Direct reduction of graphene oxide films into highly conductive and flexible graphene films by hydrohalic acids. Carbon 48:4466–4474. https://doi.org/10.1016/j.carbon.2010.08.006

Poh HL, Šaněk F, Ambrosi A, Zhao G, Sofer Z, Pumera M (2012) Graphenes prepared by Staudenmaier, Hofmann and Hummers methods with consequent thermal exfoliation exhibit very different electrochemical properties. Nanoscale 4:3515–3522. https://doi.org/10.1039/C2NR30490B

Raghavan N, Thangavel S, Sivalingam Y, Venugopal G (2018) Investigation of photocatalytic performances of sulfur based reduced graphene oxide-TiO_2 nanohybrids. Appl Surf Sci 449:712–718. https://doi.org/10.1016/j.apsusc.2018.01.043

Rahimi K, Zafarkish H, Yazdani A (2018) Reduced graphene oxide can activate the sunlight-induced photocatalytic effect of NiO nanowires. Mater Design 144:214–221. https://doi.org/10.1016/j.matdes.2018.02.030

Raveendran S, Chauhan N, Nakajima Y, Toshiaki H, Kurosu S, Tanizawa Y, Tero R, Yoshida Y, Hanajiri T, Maekawa T, Ajayan PM, Sandhu A, Kumar S (2013) Ecofriendly route for the synthesis of highly conductive graphene using extremophiles for green electronics and bioscience. Part Part Syst Char 30:573–578. https://doi.org/10.1002/ppsc.201200126

Salas EC, Sun Z, Luttge A, Tour JM (2010) Reduction of graphene oxide via bacterial respiration. ACS Nano 4:4852–4856. https://doi.org/10.1021/nn101081t

Segundo EH, Fontana LC, Recco AAC, Scholtz JS, Nespolo Vomstein MA, Becker D (2018) Graphene nanosheets obtained through graphite powder exfoliation in pulsed underwater electrical discharge. Mater Chem Phys 217:1–4. https://doi.org/10.1016/j.matchemphys.2018.06.036

Shin HJ, Kim KK, Benayad A, Yoon SM, Park HK, Jung IS, Jin MH, Jeong HK, Kim JM, Choi JY, Lee YH (2009) Efficient reduction of graphite oxide by sodium borohydride and its effect on electrical conductance. Adv Funct Mater 19:1987–1992. https://doi.org/10.1002/adfm.200900167

Shubha P, Namratha K, Aparna HS, Ashok NR, Mustak MS, Chatterjee J, Byrappa K (2017) Facile green reduction of graphene oxide using Ocimum sanctum hydroalcoholic extract and evaluation of its cellular toxicity. Mater Chem Phys 198:66–72. https://doi.org/10.1016/j.matchemphys.2017.05.062

Singh V, Joung D, Zhai L, Das S, Khondaker SI, Seal S (2011) Graphene based materials: past, present and future. Prog Mater Sci 56:1178–1271. https://doi.org/10.1016/j.pmatsci.2011.03.003

Singh M, Kaushal S, Singh P, Sharma J (2018) Boron doped graphene oxide with enhanced photocatalytic activity for organic pollutants. J Photoch Photobio A 364:130–139. https://doi.org/10.1016/j.jphotochem.2018.06.002

Soldano C, Mahmood A, Dujardin E (2010) Production, properties and potential of graphene. Carbon 48:2127–2150. https://doi.org/10.1016/j.carbon.2010.01.058

Stankovich S, Piner RD, Chen X, Wu N, Nguyen ST, Ruoff RS (2006) Stable aqueous dispersions of graphitic nanoplatelets via the reduction of exfoliated graphite oxide in the presence of poly (sodium 4-styrenesulfonate). J Mater Chem 16:155–158. https://doi.org/10.1039/B512799H

Stankovich S, Dikin DA, Piner RD, Kohlhaas KA, Kleinhammers A, Jia Y, Wu Y, Nguyen ST, Ruoff RS (2007) Synthesis of graphene-based nanosheets via chemical reduction of exfoliated graphite oxide. Carbon 45:1558–1565. https://doi.org/10.1016/j.carbon.2007.02.034

Staudenmaier L (1898) Verfahren zur Darstellung der Graphitsäure. Chem Ber 31:1481–1487. https://doi.org/10.1002/cber.19980310237

Suresh D, Nethravathi PC, Udayabhanu NH, Sharma SC (2015a) Spinach assisted green reduction of graphene oxide and its antioxidant and dye absorption properties. Ceram Int 41:4810–4813. https://doi.org/10.1016/j.ceramint.2014.12.036

Suresh D, Udayabhanu, Pavan Kumar MA, Nagabhushana H, Sharma SC (2015b) Cinnamon supported facile green reduction of graphene oxide, its dye elimination and antioxidant activities. Mater Lett 151:93–95. https://doi.org/10.1016/j.matlet.2015.03.035

Suresh D, Udayabhanu NH, Sharma SC (2015c) Clove extract mediated facile green reduction of graphene oxide, its dye elimination and antioxidant properties. Mater Lett 142:4–6. https://doi.org/10.1016/j.matlet.2014.11.073

Sykam N, Madhavi V, Rao GM (2018) Rapid and efficient green reduction of graphene oxide for outstanding supercapacitors and dye adsorption applications. J Environ Chem Eng 6:3223–3232. https://doi.org/10.1016/j.jece.2018.05.003

Tang S, Jin S, Zhang R, Liu Y, Wang J, Hu Z, Lu W, Yang S, Qiao W, Ling L, Jin M (2019) Effective reduction of graphene oxide via a hybrid microwave heating method by using mildly reduced graphene oxide as a susceptor. Appl Surf Sci 473:222–229. https://doi.org/10.1016/j.apsusc.2018.12.096

Thakur S, Karak N (2012) Green reduction of graphene oxide by aqueous phytoextracts. Carbon 50:5331–5339. https://doi.org/10.1016/j.carbon.2012.07.023

Tien HM, Luan VH, Lee TK, Kong BS, Chung JS, Kim EJ, Hur SH (2012) Enhanced solvothermal reduction of graphene oxide in a mixed solution of sulfuric acid and organic solvent. Chem Eng J 211–212:97–103. https://doi.org/10.1016/j.cej.2012.09.046

Toh SY, Loh KS, Kamarudin SK, Daud WRW (2014) Graphene production via electrochemical reduction of graphene oxide: synthesis and characterisation. Chem Eng J 251:422–434. https://doi.org/10.1016/j.cej.2014.04.004

Traversi F, Raillon C, Benameur SM, Liu K, Khlybov S, Tosun M, Krasnozhon D, Kis A, Radenovic A (2013) Detecting the translocation of DNA through a nanopore using graphene nanoribbons. Nat Nanotechnol 8:939–945. https://doi.org/10.1038/nnano.2013.240

Trenczek-Zajac A, Banas J, Radecka M (2016) TiO_2-based photoanodes modified with GO and MoS_2 layered materials. RSC Adv 6:102886. https://doi.org/10.1039/c6ra22979d

Trusovas R, Ratautas K, Raciukaitis G, Barkauskas J, Stankeviciene I, Niaura G, Mazeikiene R (2013) Reduction of graphite oxide to graphene with laser irradiation. Carbon 52:574–582. https://doi.org/10.1016/j.carbon.2012.10.017

Tsang CHA, Huang H, Xuan J, Wang H, Leung DYC (2020) Graphene materials in green energy applications: recent development and future perspective. Renew Sust Energy Rev 27:109656. https://doi.org/10.1016/j.rser.2019.109656

Wang K, Xu M, Shrestha M, Gu Z, Fan Q (2015) Plasma-assisted fabrication of graphene in ambient temperature for symmetric supercapacitors application. Mater Eletron 26:4810–4815. https://doi.org/10.1016/j.mtener.2017.03.001

Wang J, Salihi EC, Šiller L (2017) Green reduction of graphene oxide using alanine. Mater Sci Eng, C 72:1–6. https://doi.org/10.1016/j.msec.2016.11.017

Wei M, Qiao L, Zhan H, Karakalos S, Ma K, Fu Z, Swihart MT, Wu G (2017) Engineering reduced graphene oxides with enhanced electrochemical properties through multiple-step reductions. Electrochimi Acta 258:735–743. https://doi.org/10.1016/j.electacta.2017.11.120

Williams G, Seger B, Kamat PV (2008) TiO_2-graphene nanocomposites. UV-assisted photocatalytic reduction of graphene oxide. ACS Nano 7:1487–1491. https://doi.org/10.1021/nn800251f

Wu Z, Ren W, Gao L, Liu B, Jiang C, Cheng H (2009) Synthesis of high-quality graphene with a pre-determined number of layers. Carbon 47:493–499. https://doi.org/10.1016/j.carbon.2008.10.031

Wu P, He J, Chen L, Wu Y, Li H, Zhu H, Li H, Zhu W (2018) Few-layered graphene via gas-driven exfoliation for enhanced supercapacitive performance. J Energy Chem 27:1509–1515. https://doi.org/10.1016/j.jechem.2017.09.018

Xing F, Guan L, Li Y, Jia C (2016) Biosynthesis of reduced graphene oxide nanosheets and their in vitro cytotoxicity against cardiac cell lines of *Catla catla*. Environ Toxicol Phar 48:110–115. https://doi.org/10.1016/j.etap.2016.09.022

Xu C, Yuan RS, Wang X (2014) Selective reduction of graphene oxide. New Carbon Mater 29:61–66. https://doi.org/10.1016/S1872-5805(14)60126-8

Xu C, Shi X, Ji A, Shi L, Zhou C, Cui Y (2015) Fabrication and characteristics of reduced graphene oxide produced with different green reductants. PLoS ONE 10:1–15. https://doi.org/10.1371/journal.pone.0144842

Xu B, Wang H, Zhu Q, Sun N, Anasori B, Hu L, Wang F, Guan Y, Gogotsi Y (2018) Reduced graphene oxide as a multi-functional conductive binder for supercapacitor electrodes. Energy Storage Mater 12:128–136. https://doi.org/10.1016/j.ensm.2017.12.006

Yang Z, Zheng Q, Qiu H, Li J, Yang J (2015) A simple method for the reduction of graphene oxide by sodium borohydride with $CaCl_2$ as a catalyst. New Carbon Mater 30:41–47. https://doi.org/10.1016/S1872-5805(15)60174-3

Yang W, Li Y, Lee Y (2016) Synthesis of r-GO/TiO_2 composites via the UV-assisted photocatalytic reduction of graphene oxide. Appl Surf Sci 380:249–256. https://doi.org/10.1016/j.apsusc.2016.01.118

Yang C, Gong J, Zeng P, Yang X, Liang R, Ou Q, Zhang S (2018a) Fast room-temperature reduction of graphene oxide by methane/argon plasma for flexible electronics. Appl Surf Sci 452:481–486. https://doi.org/10.1016/j.apsusc.2018.04.272

Yang C, Tseng S, Chen Y (2018b) Laser-induced reduction of graphene oxide powders by high pulsed ultraviolet laser irradiations. Appl Surf Sci 444:578–583. https://doi.org/10.1016/j.apsusc.2018.03.090

Yaragalla S, Rajendran R, Jose J, AlMaadeed MA, Kalarikkal N, Thomas S (2017) Preparation and characterization of green graphene using grape seed extract for bioapplications. Appl Surf Sci 406:312–318. https://doi.org/10.1016/j.msec.2016.04.050

Yu YY, Kang BH, Lee YD, Lee SB, Ju BK (2013) Effect of fluorine plasma treatment with chemically reduced graphene oxide thin films as hole transport layer in organic solar cells. Appl Surf Sci 287:91–96. https://doi.org/10.1016/j.apsusc.2013.09.078

Zhang X, Feng Y, Lv P, Shen Y, Feng W (2010a) Enhanced reversible photoswitching of azobenzene-functionalized graphene oxide hybrids. Langmuir 26:18508–18511. https://doi.org/10.1021/la1037537

Zhang J, Yang H, Shen G, Cheng P, Zhang J, Guo S (2010b) Reduction of graphene oxide via L-ascorbic acid. Chem Commun 46:1112–1114. https://doi.org/10.1039/B917705A

Zhang X, Li K, Li H, Lu J (2013a) Dipotassium hydrogen phosphate as reducing agent for the efficient reduction of graphene oxide nanosheets. J Colloid Interface Sci 409:1–7. https://doi.org/10.1016/j.jcis.2013.07.021

Zhang H, Yu X, Guo D, Qu B, Zhang M, Li Q, Wang T (2013b) Synthesis of bacteria promoted reduced graphene oxide-nickel sulfide networks for advanced supercapacitors. ACS Appl Mater Interface 5:7335–7340. https://doi.org/10.1021/am401680m

Zhang X, Li K, Li H, Lu J, Fu Q, Chu Y (2014a) Graphene nanosheets synthesis via chemical reduction of graphene oxide using sodium acetate trihydrate solution. Synth Metals 193:132–138. https://doi.org/10.1016/j.synthmet.2014.04.007

Zhang Y, Guo L, Xia H, Chen Q, Feng J, Sun H (2014b) Photoreduction of graphene oxides: methods, properties, and applications. Adv Opt Mater 2:10–28. https://doi.org/10.1002/adom.201300317

Zhao J, Pei S, Ren W, Gao L, Cheng H (2010) Efficient preparation of large-area graphene oxide sheets for transparent conductive films. ACS Nano 4:5245–5252. https://doi.org/10.1021/nn1015506

Zhou Y, Bao Q, Tang LAL, Zhong Y, Loh KP (2009) Hydrothermal dehydration for the "green" reduction of exfoliated graphene oxide to graphene and demonstration of tunable optical limiting properties. Chem Mater 21:2950–2956. https://doi.org/10.1021/cm9006603

Zhou Y, Bao Q, Varghese B, Tang LAL, Tan CK, Sow CH, Loh KP (2010) Microstructuring of graphene oxide nanosheets using direct laser writing. Adv Mater 22:67–71. https://doi.org/10.1002/adma.200901942

Zhou D, Cheng Q, Han B (2011) Solvothermal synthesis of homogeneous graphene dispersion with high concentration. Carbon 49:3920–3927. https://doi.org/10.1016/j.carbon.2011.05.030

Zhu C, Guo S, Fang Y, Dong S (2010) Reducing sugar: new functional molecules for the green synthesis of graphene nanosheets. ACS Nano 4:2429–2437. https://doi.org/10.1021/nn1002387

Zou X, Zhang L, Wang Z, Luo Y (2016) Mechanisms of the antimicrobial activities of graphene materials. J Am Chem Soc 138:2064–2077. https://doi.org/10.1021/jacs.5b11411